Zagros J. Appl. Math. & Data. Anal.

Available online at https://zjamda.abru.ac.ir/
ISSN 0000-0000
Vol. 1, No. 2, 2025, 71–87
Research Article

Solving the Generalized Nonlinear Schrödinger Equation with Four-Wave Mixing: Insights into Soliton Dynamics and Interactions

Dean Chou
[1]Department of Biomedical Engineering, National Cheng Kung University, Tainan 701401, Taiwan.
[2]Miin Wu School of Computing, National Cheng Kung University, Tainan 701401, Taiwan.
[3] Academy of Innovative Semiconductor and Sustainable Manufacturing,
National Cheng Kung University, Tainan 701401, Taiwan.
[4]National Center for High-performance Computing, Hsinchu 300092, Taiwan.

Hamood Ur Rehman
Department of Mathematics, University of Okara, Okara, Pakistan.

Ifrah Iqbal
Department of Mathematics, University of Okara, Okara, Pakistan.

Mir Sajjad Hashemi *
Department of Mathematics, Basic Science Faculty, University of Bonab, Bonab, Iran.

Mohammad Mirzazadeh
Department of Engineering Sciences, Faculty of Technology and Engineering,
East of Guilan, University of Guilan, Rudsar-Vajargah, Iran.

Mustafa Bayram
Computer Engineering, Biruni University, Istanbul, Turkey.

Abstract

Abstract: Soliton solutions for the generalized nonlinear Schrödinger equation with four-wave mixing, which effectively characterize soliton propagation in birefringent fiber, have been introduced in this study by using three noteworthy and advanced methodologies. The speed and

*Corresponding author: hashemi_math396@yahoo.com

direction of soliton propagation, along with the mitigation of interactions between solitons, are influenced by the four-wave mixing and other parameters embedded in the proposed model. These parameters play a crucial role in governing the dynamics of the resultant solitons. Three prominent methodologies considered for this application include the method $\left(\frac{1}{\chi(\zeta)}, \frac{\chi'(\zeta)}{\chi(\zeta)}\right)$, the modified extended tanh method (METM), and the new Kudryashov's method. All three techniques have been sequentially applied to the proposed model with successful implementation. As a result, dark, bright, periodic singular, singular and combined dark-singular solutions are obtained. Furthermore, an analysis of the dynamics of these solutions is conducted through graphical representations. The significance of our findings lies in their potential to enhance our understanding and prediction of wave phenomena emerging in nonlinear wave fields.
Keywords: Nonlinear Schrödinger equation (NLSE), Four-wave mixing, Birefringent fiber, Optical Solitons.

1 Introduction

With the remarkable advancements in information technology and the escalating market demand, particularly exacerbated by the global impact of COVID-19 in recent years, contemporary society is increasingly reliant on communication. This surge in dependence has propelled the evolution of optical fiber communication towards achieving higher speeds and larger capacities. Optical fiber communication has now established itself as the primary transmission mode for communication networks, owing to its impressive attributes such as high transmission capacity, minimal signal loss, and a broad frequency band. Optical solitons, in this context, emerge as the optimal information carriers within fiber optic communications. Physically, optical solitons possess the unique ability to maintain the waveform and speed of optical fiber transmission unchanged, representing a distinctive outcome of non-linear optical effects. Consequently, optical solitons are hailed as one of the most promising transmission modes for the next generation of communication systems [1, 2, 3, 4]. From a mathematical perspective, optical solitons manifest as integrable solutions to certain non-linear partial differential equations. Investigating the exact solutions of these mathematical models stands at the forefront of this field, signifying a highly significant frontier [5, 6, 7, 8, 9, 10].

In the realm of optical fiber communication, equations of the NLSE have garnered considerable attention among researchers [11, 12, 13]. Originating in the 1850s and 1860s, the NLSE found its initial application in examining the two-dimensional self-focusing phenomenon observed in strong beams within weakly interacting non-ideal Bose gases and nonlinear media. Functioning as a comprehensive equation elucidating the propagation of wave packets in weakly nonlinear mediums, the NLSE holds paramount importance in the exploration of nonlinear physics. The investigation of solitons in birefringent fibers involves the examination of different non-linearity laws [14]. These criteria, dictating the conditions for the presence of solitons, are also acknowledged as constraining factors in the study.

To provide a precise depiction of specific nonlinear phenomena, we extend the NLSE to the coupled NLSEs, stand as fundamental models for elucidating nonlinear phenomena and find widespread application in various scientific domains, including plasma physics, nonlinear optics, condensed matter physics, and biological physics among others. Within the realm of nonlinear optics, coupled NLSE are frequently employed to elucidate the propagation dynamics of optical solitons in diverse mediums such as multimode fibers, birefringence fibers, and optical fiber arrays [15, 16]. The nonlinear effects can be categorized into four-wave mixing (FWM), self-phase modulation (SPM) and

cross-phase modulation (CPM). Notably, FWM emerges as the most impactful on optical systems. Considering these dynamics, we propose a generalized coupled NLSE incorporating the influential FWM effect to elucidate the behavior of optical solitons within a birefringent fiber [17] and read as

$$\iota Q_t + Q_{xx} + Q_{yy} + 2(a|Q|^2 + c|R|^2 + bQR^* + b^*Q^*R)Q = 0, \tag{1}$$

$$\iota R_t + R_{xx} + R_{yy} + 2(a|Q|^2 + c|R|^2 + bQR^* + b^*Q^*R)R = 0. \tag{2}$$

Here, the variables $Q(x, y, t)$ and $R(x, y, t)$, represent the envelopes characterizing the two circularly polarized waves. a and c are real constants reflecting SPM and CPM, b is a complex constant representing the FWM effect, and the symbol "*" denotes a complex conjugate.
Analytical techniques aim to unveil precise mathematical solutions for partial differential equations (PDEs). However, the inherent complexity of NLPDEs often necessitates the pursuit of simpler analytical solutions. Traveling wave methods involve the application of specific strategies to discern exact solutions for particular PDEs, emphasizing solutions that exhibit characteristic traveling wave properties. Notable approaches in this realm such as Kudryashov's method [18, 19], the extended hyperbolic function method [20, 21, 22, 23, 24], mapping method [25, 26, 27, 28], Sardar sub-equation method [29, 30], Jacobi's elliptic function [31, 32], Bernoulli sub- ODE method [33, 34], new extended direct algebraic method [35, 36], and, ϕ^6-expansion method [37]. In this study three different approaches namely $\left(\frac{1}{\chi(\zeta)}, \frac{\chi'(\zeta)}{\chi(\zeta)}\right)$ [38], the METM [39] and the new Kudryashov's method [40] are applied to extract the solutions of governed equation.
The remaining layout of paper is as follow: The mathematical analysis of paper is given 2. Section 3, 4, 5 give the methodology of three approaches along solutions. Section 6 explains the results and discussion of findings and last section is dedicated to the conclusion of the paper.

2 Mathematical Analysis

Suppose the transformations

$$Q(x, y, t) = q(\zeta)e^{\iota\phi}, \quad R(x, y, t) = r(\zeta)e^{\iota\phi}, \tag{3}$$

where $\zeta = x + y - vt, \quad \phi = -k_1x - k_2y + wt + \vartheta$. By inserting (3) into (1) and (2), we get the following real parts

$$-wq + 2q'' - (k_1^2 + k_2^2)q + 2(aq^3 + cqr^2 + bq^2r + b^*q^2r) = 0, \tag{4}$$

$$-wr + 2r'' - (k_1^2 + k_2^2)r + 2(aq^2r + cr^3 + bqr^2 + b^*qr^2) = 0, \tag{5}$$

and the imaginary parts are

$$-vq' - 2(k_1 + k_2)q' = 0, \Rightarrow v = -2(k_1 + k_2), \tag{6}$$

$$-vr' - 2(k_1 + k_2)r' = 0, \Rightarrow v = -2(k_1 + k_2). \tag{7}$$

Now, suppose $r = \mu q$, the real parts yield the same equation

$$2q'' - (k_1^2 + k_2^2 + w)q + 2(a + c\mu^2 + b\mu + b^*\mu)q^3 = 0. \tag{8}$$

3 Description of $\left(\frac{1}{\chi(\zeta)}, \frac{\chi'(\zeta)}{\chi(\zeta)}\right)$ method

Assume the solution of (8) is

$$q(\zeta) = c_0 + \sum_{i=1}^{m} \frac{c_i + d_i \chi'(\zeta)^i}{\chi(\zeta)^i}, \tag{9}$$

where c_0, c_i and d_i $(i = 1, 2...m)$ are constants. The value of m can be determined using the homogeneous balancing rule, and $\chi(\zeta)$ satisfies the following ODE:

$$\chi'(\zeta)^2 = \chi(\zeta)^2 - \varrho, \tag{10}$$

where

$$\chi(\zeta) = ge^{\zeta} + \frac{\varrho}{4ge^{\zeta}}. \tag{11}$$

By substituting (9) and (10) into (8), we obtain a system of equations, which, when solved, yields the values of the constants.

4 Application of $\left(\frac{1}{\chi(\zeta)}, \frac{\chi'(\zeta)}{\chi(\zeta)}\right)$ method

The homogeneous balance rule gives $m = 1$.

$$q(\zeta) = c_0 + \frac{c_1 + d_1 \chi'(\zeta)}{\chi(\zeta)}. \tag{12}$$

Now, by inserting (12) along (10) and (11) into (8) , the system of equations is attained which yields the values of constants.

Set 1 $\left\{c_0 = 0, \quad c_1 = 0, \quad w = \left(-k_1^2 - k_2^2 - 4\right), \quad b = \dfrac{-ad_1^2 - c\mu^2 d_1^2 - b^*\mu d_1^2 - 2}{\mu d_1^2}\right\}.$

By using these values of constants along (11) in (12) and with the help of $r = \mu q$ we, can get the solution of (1) and (2).

$$Q_{1,*}(x, y, t) = \left(\frac{d_1\left(4g^2e^{2\zeta} - \varrho\right)}{4g^2e^{2\zeta} + \varrho}\right) e^{\iota\phi},$$
$$P_{1,*}(x, y, t) = \mu\left(\frac{d_1\left(4g^2e^{2\zeta} - \varrho\right)}{4g^2e^{2\zeta} + \varrho}\right) e^{\iota\phi}.$$

If we put $\varrho = \pm 4g^2$, we have the following solutions

$$Q_{1,1}(x, y, t) = \left(d_1 tanh(\zeta)\right) e^{\iota\phi},$$
$$P_{1,1}(x, y, t) = \mu\left(d_1 tanh(\zeta)\right) e^{\iota\phi}.$$

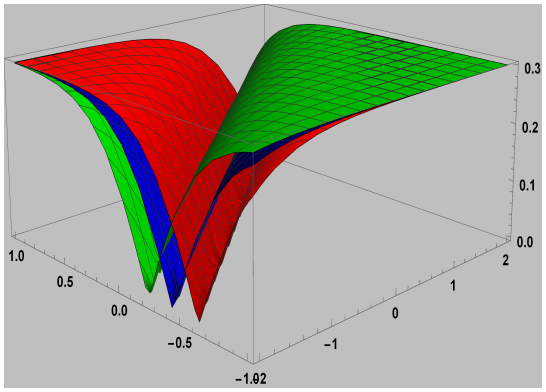

(a) y=0.5 y=1 y=1.5

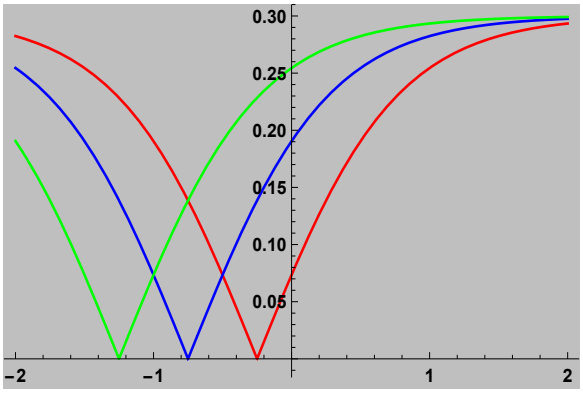

(b) y=0.5 y=1 y=1.5

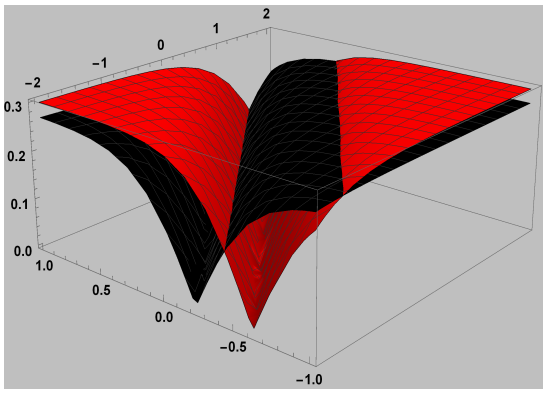

(c) $Q_{1,1}$, $P_{1,1}$

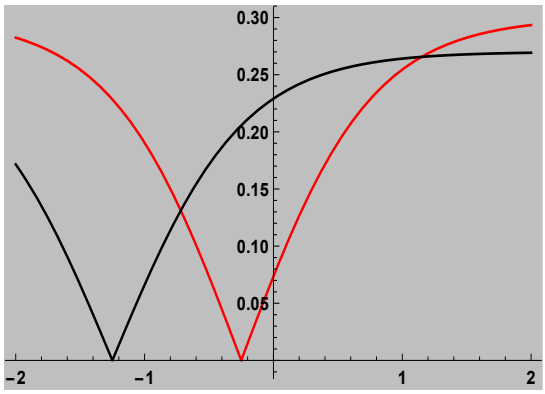

(d) $Q_{1,1}$, $P_{1,1}$

Figure 1: Graphics of $Q_{1,1}$ and $P_{1,1}$ with the following parameters $k_1 = 1,\ k_2 = 1.5,\ d_1 = 0.3,\ v = 2.5,$ and $\mu = 0.8$.

$$Q_{1,2}(x,y,t) = (d_1 coth(\zeta))\, e^{\iota\phi},$$
$$P_{1,2}(x,y,t) = \mu\,(d_1 coth(\zeta))\, e^{\iota\phi}.$$

Set 2 $\left\{c_0 = 0,\ \ d_1 = 0,\ \ w = \left(-k_1^2 - k_2^2 - 2\right),\ \ b = \dfrac{-ac_1^2 - c\mu^2 c_1^2 - b^*\mu c_1^2 - 2}{\mu c_1^2}\right\}.$

The solutions obtained from above set are

$$Q_{1,**}(x,y,t) = \left(\frac{4gc_1 e^{\zeta}}{4g^2 e^{2\zeta} + \varrho}\right) e^{\iota\phi},$$
$$P_{1,**}(x,y,t) = \mu\left(\frac{4gc_1 e^{\zeta}}{4g^2 e^{2\zeta} + \varrho}\right) e^{\iota\phi}.$$

If we put $\varrho = \pm 4g^2$, we have the following solutions

$$Q_{1,2}(x,y,t) = \left(\frac{c_1 \text{sech}(\zeta)}{2g}\right) e^{\iota\phi},$$
$$P_{1,2}(x,y,t) = \mu \left(\frac{c_1 \text{sech}(\zeta)}{2g}\right) e^{\iota\phi}.$$

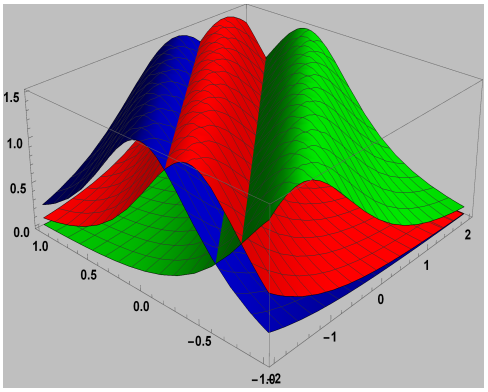

(a) y=1 y=2.5 y=-1

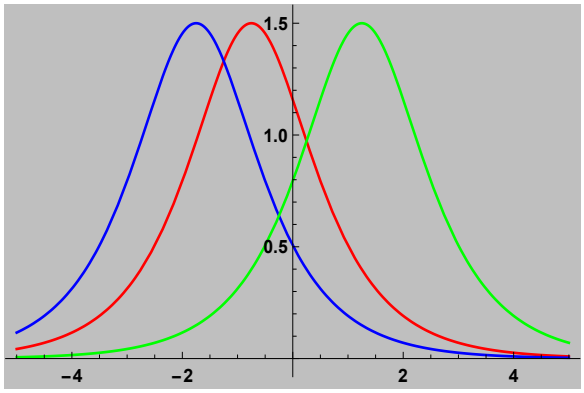

(b) y=1 y=2.5 y=-1

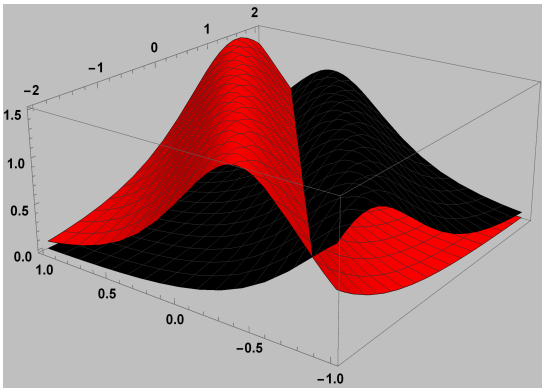

(c) $Q_{1,3}$, $P_{1,3}$

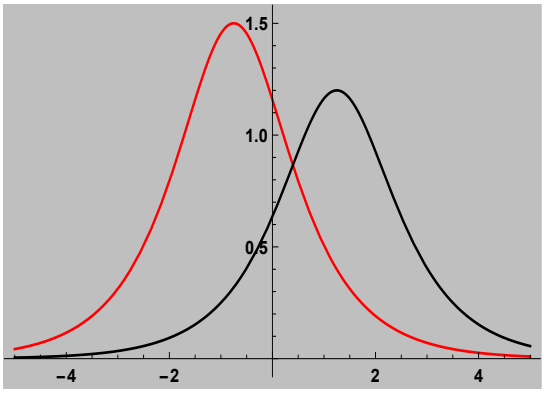

(d) $Q_{1,3}$, $P_{1,3}$

Figure 2: Graphics of $Q_{1,3}$ and $P_{1,3}$ with the following parameters $g = 0.1$. $k_1 = 1$, $k_2 = 1.5$, $c_1 = 0.3$, $v = 2.5$, *and* $\mu = 0.8$

$$Q_{1,3}(x,y,t) = \left(\frac{c_1 \text{csch}(\zeta)}{2g}\right) e^{\iota\phi},$$
$$P_{1,3}(x,y,t) = \mu \left(\frac{c_1 \text{csch}(\zeta)}{2g}\right) e^{\iota\phi}.$$

5 METM

Let us assume the solution of (8) in the form of

$$q(\varsigma) = \nu_0 + \sum_{j=1}^{N} \nu_j Z^j(\zeta) + \sum_{j=1}^{N} \frac{V_j}{Z^j(\zeta)}. \tag{13}$$

The function $Z^j(\varsigma)$ satisfies the following equation

$$Z'(\zeta) = Z^2(\zeta) + h. \tag{14}$$

The solution of (14) can be written as:
(Family 1): If $h < 0$, then

$$Z_1(\zeta) = -\sqrt{-h}tanh(-\sqrt{-h}\zeta),$$
$$Z_2(\zeta) = -\sqrt{-h}coth(-\sqrt{-h}\zeta).$$

(Family 2): If $h > 0$, then

$$Z_3(\zeta) = \sqrt{h}tan(\sqrt{h}\zeta),$$
$$Z_4(\zeta) = -\sqrt{h}cot(\sqrt{h}\zeta).$$

(Family 3): If $h = 0$, then

$$Z_5(\varsigma) = -\frac{1}{\varsigma}.$$

By applying (13) and (14) to (8), we derive a system of equations, and solving this system provides the values of the constants.

5.1 Application of METM

Now, from (13), suppose the following solutions

$$q(\zeta) = \nu_0 + \nu_1 Z(\zeta) + \frac{V_1}{Z(\zeta)}. \tag{15}$$

By substituting (15) and (14) into (8), we derived the following constants.

$$\textbf{Set 1} \quad \left\{ \nu_0 = 0, \quad \nu_1 = \nu_1, a = \frac{-b\nu_1^2\mu + \nu_1^2(-c)\mu^2 - \nu_1^2 b^*\mu - 2}{\nu_1^2}, V_1 = 0 \right\}.$$

(Case 1): If $h < 0$, then

$$Q_{2,1}(x,y,t) = \left(\nu_1 \left(-\sqrt{-h}tanh(-\sqrt{-h}\zeta\right)\right) e^{\iota\phi},$$
$$P_{2,1}(x,y,t) = \mu \left(\nu_1 \left(-\sqrt{-h}tanh(-\sqrt{-h}\zeta\right)\right) e^{\iota\phi}.$$

$$Q_{2,2}(x,y,t) = \left(\nu_1\left(-\sqrt{-h}coth(-\sqrt{-h}\zeta\right)\right)e^{\iota\phi},$$
$$P_{2,2}(x,y,t) = \mu\left(\nu_1\left(-\sqrt{-h}coth(-\sqrt{-h}\zeta\right)\right)e^{\iota\phi}.$$

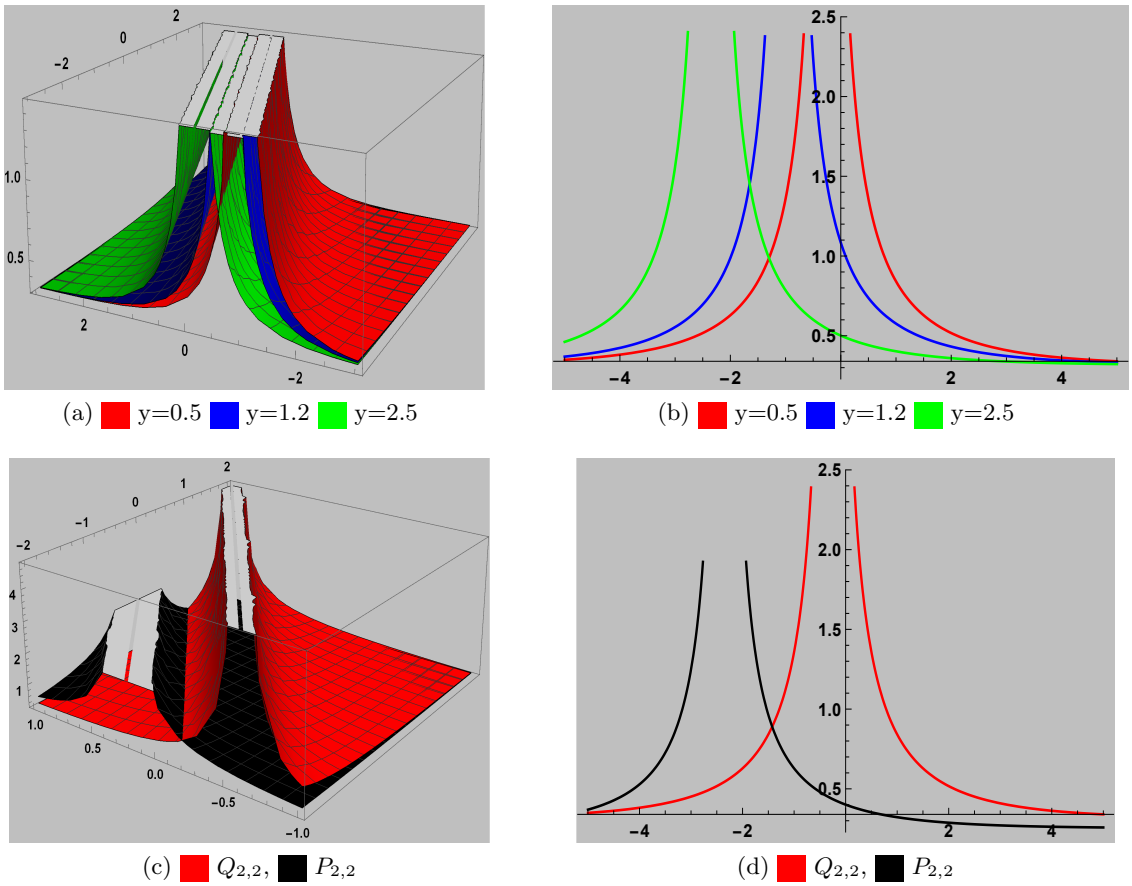

Figure 3: Graphics of $Q_{2,2}$ and $P_{2,2}$ with the following parameters $h = -0.1,\ \nu_1 = 0.1,\ k_1 = 1,\ k_2 = 1.5,\ v = 2.5$, and $\mu = 0.8$.

(Case 2): If $h > 0$, then

$$Q_{2,3}(x,y,t) = \left(\nu_1\left(\sqrt{h}tan(\sqrt{h}\zeta\right)\right)e^{\iota\phi},$$
$$P_{2,3}(x,y,t) = \mu\left(\nu_1\left(\sqrt{h}tan(\sqrt{h}\zeta\right)\right)e^{\iota\phi}.$$

$$Q_{2,3}(x,y,t) = \left(\nu_1\left(\sqrt{h}cot(\sqrt{h}\zeta\right)\right)e^{\iota\phi},$$
$$P_{2,3}(x,y,t) = \mu\left(\nu_1\left(\sqrt{h}cot(\sqrt{h}\zeta\right)\right)e^{\iota\phi}.$$

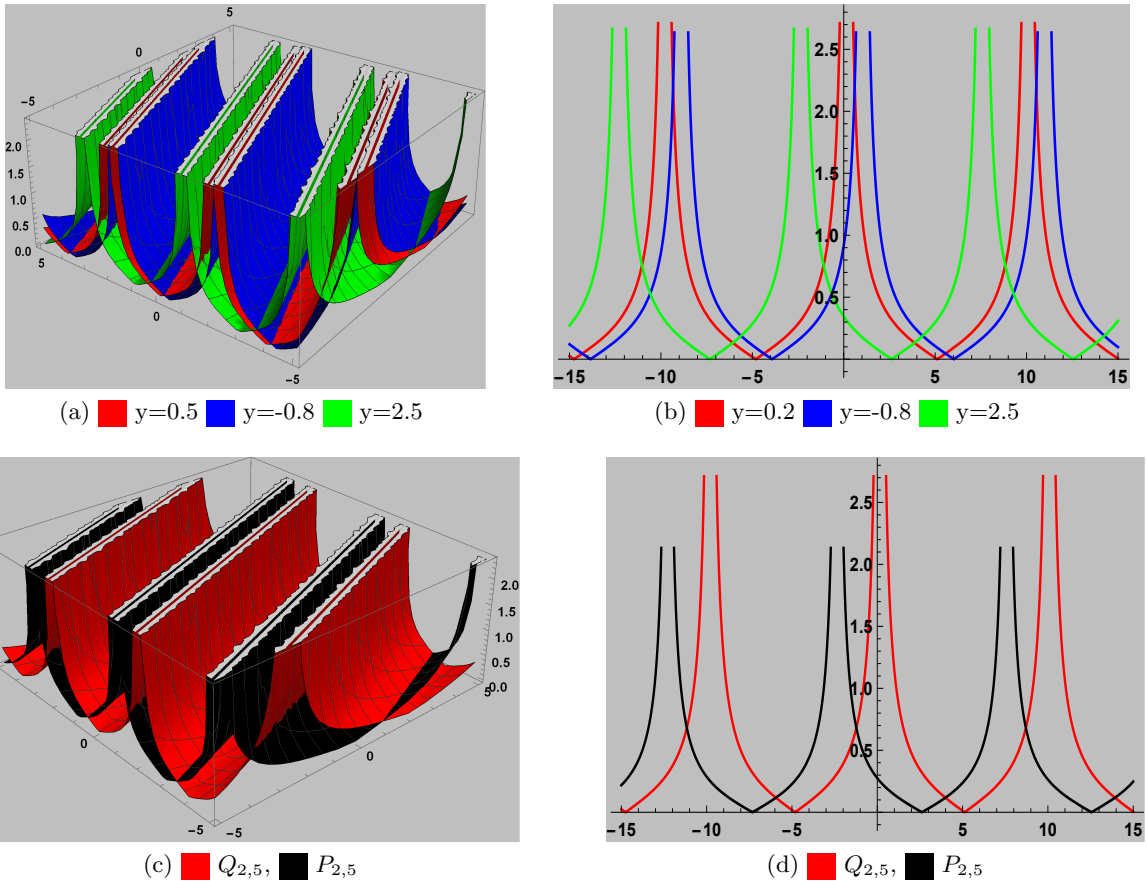

(a) y=0.5 y=-0.8 y=2.5 (b) y=0.2 y=-0.8 y=2.5

(c) $Q_{2,5}$, $P_{2,5}$ (d) $Q_{2,5}$, $P_{2,5}$

Figure 4: Graphics of $Q_{2,5}$ and $P_{2,5}$ with the following parameters $h = 0.1,\ k_1 = 1,\ k_2 = 1.5,\ \nu_1 = 0.3,\ v = 2.5,\ and\ \mu = 0.9.$

(Case 3): If $h = 0$, then

$$Q_{2,5}(x,y,t) = \left(-\frac{\nu_1}{\zeta}\right) e^{\iota\phi},$$
$$P_{2,3}(x,y,t) = \mu \left(-\frac{\nu_1}{\zeta}\right) e^{\iota\phi}.$$

Set 2 $\left\{\nu_0 = 0,, \quad V_1 = \mu_1 h, \quad w = 16h - k_1^2 - k_2^2, \quad a = \dfrac{-b\nu_1^2\mu + \nu_1^2(-c)\mu^2 - \nu_1^2 b^*\mu - 2}{\nu_1^2}\right\}.$

(Case 1): If $h < 0$, then

$$Q_{2,6}(x,y,t) = \left(\frac{\nu_1 h \coth\left(\zeta\sqrt{-h}\right) - V_1 \tanh\left(\zeta\sqrt{-h}\right)}{\sqrt{-h}}\right) e^{\iota\phi},$$
$$P_{2,6}(x,t) = \mu \left(\frac{\nu_1 h \coth\left(\zeta\sqrt{-h}\right) - V_1 \tanh\left(\zeta\sqrt{-h}\right)}{\sqrt{-h}}\right) e^{\iota\phi}.$$

$$Q_{2,7}(x,y,t) = \left(\frac{\nu_1 h \tanh\left(\zeta\sqrt{-h}\right) - V_1 \coth\left(\zeta\sqrt{-h}\right)}{\sqrt{-h}} \right) e^{\iota\phi},$$
$$P_{2,7}(x,y,t) = \mu \left(\frac{\nu_1 h \tanh\left(\zeta\sqrt{-h}\right) - V_1 \coth\left(\zeta\sqrt{-h}\right)}{\sqrt{-h}} \right) e^{\iota\phi}$$

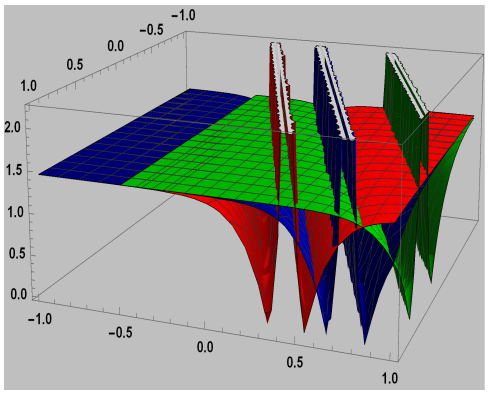

(a) y=0.1 y=0.9 y=2.1

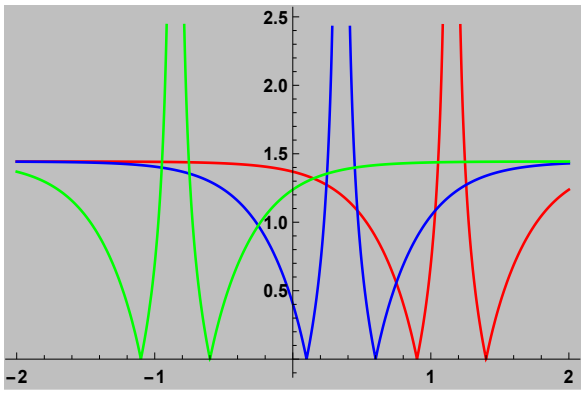

(b) y=0.1 y=-0.9 y=2.1

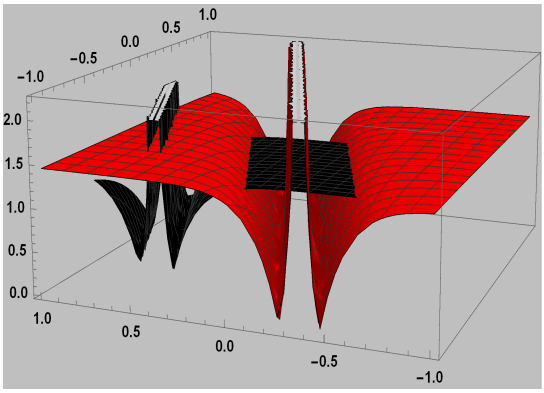

(c) $Q_{2,7}$, $P_{2,7}$

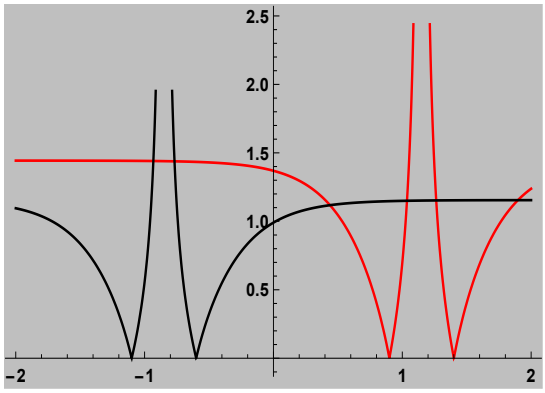

(d) $Q_{2,7}$, $P_{2,7}$

Figure 5: Graphics of $Q_{2,7}$ and $P_{2,7}$ with the following parameters $h = -0.1,\ \nu_1 = 0.1,\ k_1 = 1,\ k_2 = 1.5,\ V_1 = 0.3,\ v = 2.5$

(Case 2): If $h > 0$, then

$$Q_{2,8}(x,y,t) = \left(\frac{\nu_1 h \tan\left(\zeta\sqrt{h}\right) + V_1 \cot\left(\zeta\sqrt{h}\right)}{\sqrt{h}} \right) e^{\iota\phi},$$
$$P_{2,8}(x,y,t) = \mu \left(\frac{\nu_1 h \tan\left(\zeta\sqrt{h}\right) + V_1 \cot\left(\zeta\sqrt{h}\right)}{\sqrt{h}} \right) e^{\iota\phi}.$$

$$Q_{2,8}(x,y,t) = \left(\frac{\nu_1 h \cot\left(\zeta\sqrt{h}\right) + V_1 \tan\left(\zeta\sqrt{h}\right)}{\sqrt{h}} \right) e^{\iota\phi},$$
$$P_{2,8}(x,y,t) = \mu \left(\frac{\nu_1 h \cot\left(\zeta\sqrt{h}\right) + V_1 \tan\left(\zeta\sqrt{h}\right)}{\sqrt{h}} \right) e^{\iota\phi}.$$

6 New Kudryashov's method

Assume, the solution of (8) is

$$q(\zeta) = \sum_{k=1}^{M} h_k Y^k(\zeta), \tag{16}$$

where h_k $(k = 1, 2...M)$ are constants. The value of M can be derived using the homogeneous balancing method, and $Y(\zeta)$ denotes the following ODE:

$$Y'(\zeta)^2 = \delta^2 Y(\zeta)^2 (1 - \chi Y(\zeta)^2), \tag{17}$$

where

$$Y(\zeta) = \frac{4R}{4e^{\delta\zeta}R^2 + e^{-\delta\zeta}\chi}. \tag{18}$$

By substituting (16) and (17) into (8), we obtain a system of equations. Solving this system yields the values of the constants.

6.1 Application of new Kudryashov's method:

As homogeneous balancing rule gives $M = 1$, so we have the following solution

$$q(\zeta) = h_0 + h_1 Y(\zeta). \tag{19}$$

The subsitution of (19) along (17) into (8), yields following set of solutions

$$h_0 = 0, \quad b^* = \frac{-ah_1^2 - bh_1^2\mu + h_1^2(-c)\mu^2 + 2\delta^2\chi}{h_1^2\mu}, \quad k_2 = \sqrt{2\delta^2 - k_1^2 - w}.$$

By substituting these constant values into (19), we derive the following solutions

$$Q_{3,*}(x,y,t) = \left(\frac{4h_1 R e^{\delta\zeta}}{4R^2 e^{2\delta\zeta} + \chi} \right) e^{\iota\phi},$$
$$P_{3,*}(x,y,t) = \mu \left(\frac{4h_1 R e^{\delta\zeta}}{4R^2 e^{2\delta\zeta} + \chi} \right) e^{\iota\phi}.$$

If $\chi = \pm 4R^2$, then

$$Q_{3,1}(x,y,t) = \left(\frac{h_1 \mathrm{sech}(\zeta\delta)}{2R} \right) e^{\iota\phi},$$
$$P_{3,1}(x,y,t) = \mu \left(\frac{h_1 \mathrm{sech}(\zeta\delta)}{2R} \right) e^{\iota\phi}.$$

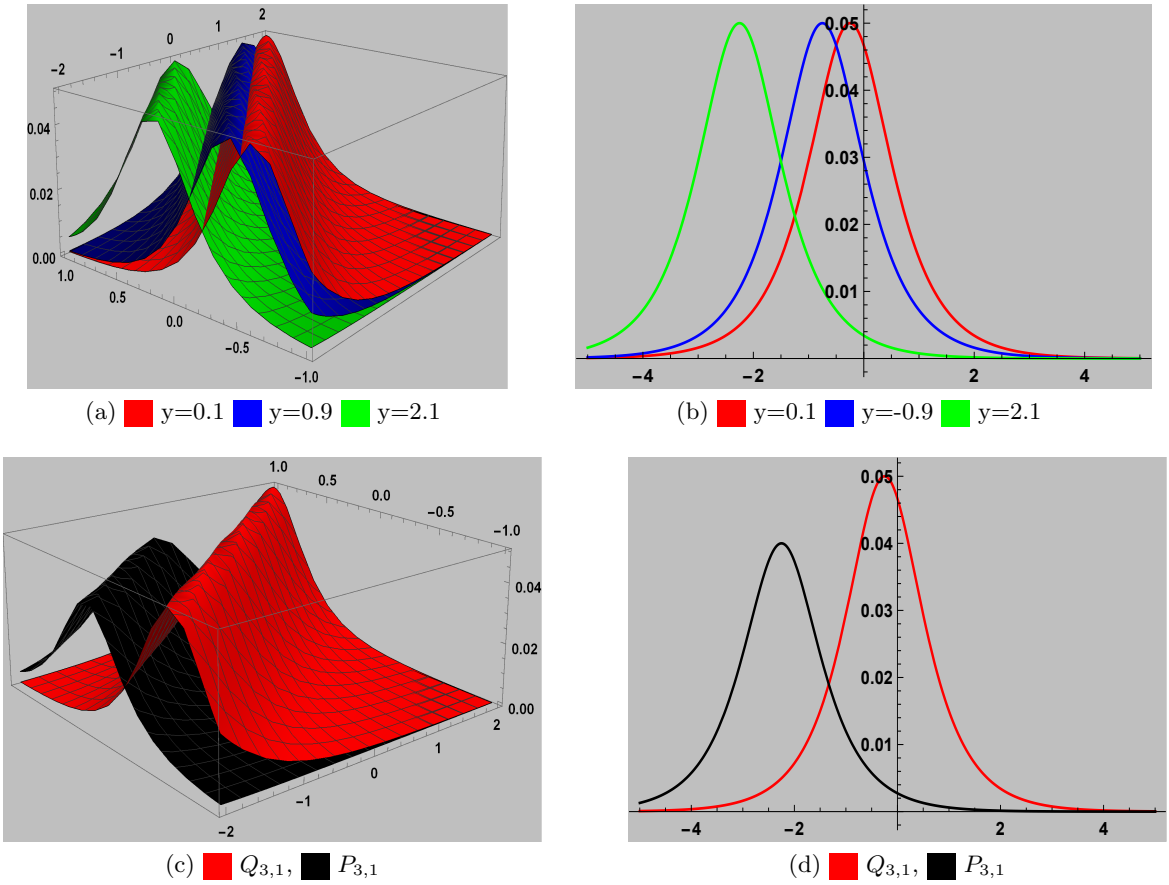

Figure 6: Graphics of $Q_{3,1}$ and $P_{3,1}$ with the following parameters $\mu = 0.1,\ h_1 = 0.1,\ k_1 = 1,\ w = 1.5,\ \delta = 0.3,\ v = 2.5,$ and R=0.5

$$Q_{4,1}(x,y,t) = \left(\frac{h_1 \text{csch}(\zeta\delta)}{2R}\right) e^{\iota\phi},$$
$$P_{4,1}(x,y,t) = \mu\left(\frac{h_1 \text{csch}(\zeta\delta)}{2R}\right) e^{\iota\phi}.$$

7 Results and Discussion:

In the current work, we utilize three different techniques to extract solutions for the governed equation. The utilization of these techniques allowed us to explore and understand the intricate dynamics of soliton propagation in birefringent fibers. Different types of solitons are obtained from these methods such as bright, dark, singular, periodic singular and combined dark-bright singular as given in Table 1.

By plotting both 3D and 2D graphs, a comparative analysis of the soliton profiles at different values of y, highlighting the shifting which show the stability and preservation of soliton amplitude and phase during propagation. This observation is significant for understanding the practical

Method	**Types of Solutions**
$\left(\frac{1}{\chi(\zeta)}, \frac{\chi'(\zeta)}{\chi(\zeta)}\right)$ method	Dark, Singular, Bright Solitons.
METM	Singular, Periodic, Dark, Combined dark-singular Solitons.
New Kudryashov's method	Bright, Singular Solitons.

Table 1: Types of Soliton Solutions

implications of the proposed model in optical fiber communication systems. An additional graph presented a comparative analysis of both soliton profiles which explains how the soliton's characteristics evolve with changes in amplitude. The findings hold significant implications in optical fiber communication as they predict and control soliton propagation in birefringent fibers for the development large-capacity communication systems.
Figure 1 provides a graphical representation of the dark soliton solutions for the solution $Q_{1,1}(x, y, t)$. In Fig 1a and Fig 1b, the 3D and 2D plots at different values of y demonstrate that the soliton propagates forward or backward while preserving its amplitude and phase. Figures 1c and 1d present the 3D and 2D comparisons of both profiles, highlighting the soliton's forward or backward transmission with varying amplitude. Moving on to Figure 2, it showcases the graphical illustrations of $Q_{1,3}(x, y, t)$, representing the bright soliton solution. Figs 2a and 2b exhibit the 3D and 2D plots at different y values, illustrating the soliton's forward or backward transmission while maintaining amplitude and phase. Figures 2c and 2d present the 3D and 2D comparisons of both profiles, emphasizing the soliton's transmission characteristics with changes in amplitude. Figure 3 focuses on $Q_{2,2}(x, y, t)$, presenting graphical illustrations of the singular soliton solution. Figs 3a and 3b display the 3D and 2D plots at varying y values, showcasing the soliton's forward or backward transmission while preserving amplitude and phase. Figures 3c and 3d provide 3D and 2D comparisons of both profiles, underlining the soliton's transmission characteristics with amplitude variations. In Figure 4, graphical illustrations of $Q_{2,5}(x, y, t)$ are presented, representing the periodic soliton solution. Figs 4a and 4b show 3D and 2D plots at different y values, illustrating the soliton's forward or backward transmission while maintaining amplitude and phase. Figures 4c and 4d offer 3D and 2D comparisons of both profiles, elucidating the soliton's transmission characteristics with amplitude changes. Figure 5 displays graphical illustrations of $Q_{2,7}(x, y, t)$ representing the dark-singular soliton solution. Figs 5a and 5b showcase the 3D and 2D plots at different y values, revealing the soliton's forward or backward transmission while preserving amplitude and phase. Figures 5c and 5d provide 3D and 2D comparisons of both profiles, emphasizing the soliton's transmission characteristics with varying amplitudes. Figure 6 illustrates graphical illustrations of $Q_{3,1}(x, y, t)$ representing the bright soliton solution. Figs 6a and 6b showcase the 3D and 2D plots at different y values, revealing the soliton's forward or backward transmission while preserving amplitude and phase. Figures 6c and 6d provide 3D and 2D comparisons of both profiles, emphasizing the soliton's transmission characteristics with varying amplitudes.

8 Conclusion

This study delves into the soliton solutions of the generalized NLSE incorporating four-wave mixing, a framework that significantly characterizes soliton propagation within birefringent fiber. Employing

three different methodologies, namely the $\left(\frac{1}{\chi(\zeta)}, \frac{\chi'(\zeta)}{\chi(\zeta)}\right)$, the METM, and new Kudryashov's method. Our investigation successfully explores the intricate dynamics of soliton behavior. The application of the three prominent methodologies leads to the derivation of diverse soliton solutions, including dark, bright, periodic singular, singular, and combined dark-singular solutions. The analysis of these solutions through graphical representations enhances our comprehension of their dynamics. A comparative analysis of the soliton profiles at different values of y, highlighting the shifting characteristics show the stability of soliton amplitude and phase during propagation, while the comparative analysis of both soliton profiles explains how the soliton's characteristics evolve with changes in amplitude. Generates dummy text. Replace with your own.

References

[1] Drazin, P. G., & Johnson, R. S. (1989). *Solitons: An introduction* (Vol. 2). Cambridge University Press.

[2] Mirzazadeh, M., Eslami, M., & Biswas, A. (2014). Dispersive optical solitons by Kudryashov's method. *Optik, 125*(23), 6874–6880.

[3] Nazarzadeh, A., Eslami, M., & Mirzazadeh, M. (2013). Exact solutions of some nonlinear partial differential equations using functional variable method. *Pramana, 81*, 225–236.

[4] Hashemi, M. S. (2024). A variable coefficient third degree generalized Abel equation method for solving stochastic Schrödinger–Hirota model. *Chaos, Solitons & Fractals, 180*, 114606.

[5] Gao, H., Kaltenbach, S., & Koumoutsakos, P. (2025). Generative learning of the solution of parametric partial differential equations using guided diffusion models and virtual observations. *Computer Methods in Applied Mechanics and Engineering, 435*, 117654.

[6] Xiang, Z., Peng, W., Yao, W., Liu, X., & Zhang, X. (2024). Solving spatiotemporal partial differential equations with physics-informed graph neural network. *Applied Soft Computing, 155*, 111437.

[7] Borgese, G., Vena, S., Pantano, P., Pace, C., Bilotta, E., et al. (2015). Simulation, modeling, and analysis of soliton waves interaction and propagation in CNN transmission lines for innovative data communication and processing. *Discrete Dynamics in Nature and Society, 2015*.

[8] Guo, S., Fritsch, A. R., Greenberg, C., Spielman, I. B., & Zwolak, J. P. (2021). Machine-learning enhanced dark soliton detection in Bose–Einstein condensates. *Machine Learning: Science and Technology, 2*(3), 035020.

[9] Eldidamony, H. A., Arnous, A. H., Mirzazadeh, M., Hashemi, M. S., & Bayram, M. (2025). Comparative approaches to solving the (2+1)-dimensional generalized coupled nonlinear Schrödinger equations with four-wave mixing. *Nonlinear Analysis: Modelling and Control, 30*, 1–25.

[10] Cinar, M., Secer, A., Hashemi, M. S., Ozisik, M., & Bayram, M. (2024). A comprehensive analysis of Fokas–Lenells equation using Lie symmetry method. *Mathematical Methods in the Applied Sciences, 47*(7), 5819–5830.

[11] Ur Rehman, H., Asjad Imran, M., Bibi, M., Riaz, M., & Akgül, A. (2021). New soliton solutions of the 2D-chiral nonlinear Schrödinger equation using two integration schemes. *Mathematical Methods in the Applied Sciences, 44*(7), 5663–5682.

[12] Sultan, A. M., Lu, D., Arshad, M., Rehman, H. U., & Saleem, M. S. (2020). Soliton solutions of higher order dispersive cubic-quintic nonlinear Schrödinger equation and its applications. *Chinese Journal of Physics, 67*, 405–413.

[13] Plastino, A. R., & Tsallis, C. (n.d.). Nonlinear Schrödinger equation in the presence of uniform acceleration. *Journal of Mathematical Physics, 54*(4).

[14] Hendi, A. A., Ouahid, L., Owyed, S., & Abdou, M. (2021). New periodic solutions for Ginzburg–Landau in three different derivatives via extended Jacobian elliptic function method. *Results in Physics, 24*, 104152.

[15] Gao, Z., Song, S., & Duan, J. (2018). The application of (2+1)-dimensional coupled nonlinear Schrödinger equations with variable coefficients in optical fibers. *Optik, 172*, 953–967.

[16] Fu, L., Li, J., Yang, H., Dong, H., & Han, X. (2023). Optical solitons in birefringent fibers with the generalized coupled space–time fractional non-linear Schrödinger equations. *Frontiers in Physics, 11*, 1108505.

[17] Wang, L., Luan, Z., Zhou, Q., Biswas, A., Alzahrani, A. K., & Liu, W. (2021). Bright soliton solutions of the (2+1)-dimensional generalized coupled nonlinear Schrödinger equation with the four-wave mixing term. *Nonlinear Dynamics, 104*, 2613–2620.

[18] Rehman, H. U., Ullah, N., & Imran, M. (2019). Highly dispersive optical solitons using Kudryashov's method. *Optik, 199*, 163349.

[19] Ryabov, P. N., Sinelshchikov, D. I., & Kochanov, M. B. (2011). Application of the Kudryashov method for finding exact solutions of the high order nonlinear evolution equations. *Applied Mathematics and Computation, 218*(7), 3965–3972.

[20] Shi, D., Rehman, H. U., Iqbal, I., Vivas-Cortez, M., Saleem, M. S., & Zhang, X. (2023). Analytical study of the dynamics in the double-chain model of DNA.

[21] Rehman, H. U., Awan, A. U., Tag-ElDin, E. M., Alhazmi, S. E., Yassen, M. F., & Haider, R. (2022). Extended hyperbolic function method for the (2+1)-dimensional nonlinear soliton equation. *Results in Physics, 40*, 105802.

[22] Hong, Z., Ji-Guang, H., Wei-Tao, W., & Hong-Yong, A. (2007). Applications of extended hyperbolic function method for quintic discrete nonlinear Schrödinger equation. *Communications in Theoretical Physics, 47*(3), 474.

[23] Ullah, N., Asjad, M. I., Muhammad, T., & Akgül, A. (n.d.). Analysis of power law non-linearity in solitonic solutions using extended hyperbolic function method.

[24] Rehman, H. U., Imran, M. A., Ullah, N., & Akgül, A. (n.d.). Exact solutions of (2+1)-dimensional Schrödinger's hyperbolic equation using different techniques. *Numerical Methods for Partial Differential Equations*.

[25] Rehman, H. U., Saleem, M. S., Zubair, M., Jafar, S., & Latif, I. (2019). Optical solitons with Biswas–Arshed model using mapping method. *Optik, 194*, 163091.

[26] Zeng, X., & Yong, X. (2008). A new mapping method and its applications to nonlinear partial differential equations. *Physics Letters A, 372*(44), 6602–6607.

[27] Mohammed, W. W., & Cesarano, C. (2023). The soliton solutions for the (4+1)-dimensional stochastic Fokas equation. *Mathematical Methods in the Applied Sciences, 46*(6), 7589–7597.

[28] Mohammed, W. W., Al-Askar, F. M., & Cesarano, C. (2022). The analytical solutions of the stochastic mKdV equation via the mapping method. *Mathematics, 10*(22), 4212.

[29] Rehman, H. U., Iqbal, I., Aiadi, S. S., Mlaiki, N., & Saleem, M. S. (2022). Soliton solutions of Klein–Fock–Gordon equation using Sardar subequation method. *Mathematics, 10*(18), 3377.

[30] Iqbal, I., Rehman, H. U., Mirzazadeh, M., & Hashemi, M. S. (2023). Retrieval of optical solitons for nonlinear models with Kudryashov's quintuple power law and dual-form nonlocal nonlinearity. *Optical and Quantum Electronics, 55*(7), 588.

[31] Liu, S., Fu, Z., Liu, S., & Zhao, Q. (2001). Jacobi elliptic function expansion method and periodic wave solutions of nonlinear wave equations. *Physics Letters A, 289*(1–2), 69–74.

[32] Allahyani, S. A., Rehman, H. U., Awan, A. U., Tag-ElDin, E. M., & Hassan, M. U. (2022). Diverse variety of exact solutions for nonlinear Gilson–Pickering equation. *Symmetry, 14*(10), 2151.

[33] Salam, M. A., Uddin, M. S., & Dey, P. (2015). Generalized Bernoulli sub-ODE method and its applications. *Annals of Pure and Applied Mathematics, 10*(1), 1–6.

[34] Zheng, B. (2011). A new Bernoulli sub-ODE method for constructing traveling wave solutions for two nonlinear equations with any order. *UPB Scientific Bulletin, Series A, 73*(3), 85–94.

[35] Rehman, H. U., Ullah, N., & Imran, M. (2021). Optical solitons of Biswas–Arshed equation in birefringent fibers using extended direct algebraic method. *Optik, 226*, 165378.

[36] Kurt, A., Tozar, A., & Tasbozan, O. (2020). Applying the new extended direct algebraic method to solve the equation of obliquely interacting waves in shallow waters. *Journal of Ocean University of China, 19*, 772–780.

[37] Shahzad, M. U., Rehman, H. U., Awan, A. U., Zafar, Z., Hassan, A. M., & Iqbal, I. (2023). Analysis of the exact solutions of nonlinear coupled Drinfeld–Sokolov–Wilson equation through φ6-model expansion method. *Results in Physics, 52*, 106771.

[38] Arnous, A. H., Nofal, T. A., Biswas, A., Yıldırım, Y., & Asiri, A. (2023). Cubic-quartic optical solitons of the complex Ginzburg–Landau equation: A novel approach. *Nonlinear Dynamics, 111*(21), 20201–20216.

[39] Zahran, E. H., & Khater, M. M. (2016). Modified extended tanh-function method and its applications to the Bogoyavlenskii equation. *Applied Mathematical Modelling, 40*(3), 1769–1775.

[40] Rehman, H. U., Said, G. S., Amer, A., Ashraf, H., Tharwat, M., Abdel-Aty, M., Elazab, N. S., & Osman, M. (2024). Unraveling the (4+1)-dimensional Davey–Stewartson–Kadomtsev–Petviashvili equation: Exploring soliton solutions via multiple techniques. *Alexandria Engineering Journal, 90*, 17–23.